FILE COPY
NO 4

RESTRICTED

Copy No. 190
RM No. L8G05

NACA RM No. L8G05

RESEARCH MEMORANDUM

FULL-SCALE INVESTIGATION OF AN EQUILATERAL TRIANGULAR WING HAVING 10-PERCENT-THICK BICONVEX AIRFOIL SECTIONS

By Edward F. Whittle, Jr., and J. Calvin Lovell

Langley Aeronautical Laboratory
Langley Field, Va.

THIS DOCUMENT ON LOAN FROM THE FILES OF
NATIONAL ADVISORY COMMITTEE FOR AERONAUTICS
LANGLEY AERONAUTICAL LABORATORY
LANGLEY FIELD, HAMPTON, VIRGINIA
RETURN TO THE ABOVE ADDRESS.

CLASSIFICATION CHANGED TO
UNCLASSIFIED
AUTHORITY CROWLEY CHANGE #1946
DATE 12-14-53 T.C.F.

NASA FILE COPY
Loan expires on last date stamped on back cover.
PLEASE RETURN TO
REPORT DISTRIBUTION SECTION
LANGLEY RESEARCH CENTER
NATIONAL AERONAUTICS AND
SPACE ADMINISTRATION
Langley Field, Virginia

CLASSIFIED DOCUMENT

This document contains classified information affecting the National Defense of the United States within the meaning of the Espionage Act, USC 50:31 and 32. Its transmission or the revelation of its contents in any manner to an unauthorized person is prohibited by law. Information so classified may be imparted only to persons in the military and naval services of the United States, appropriate civilian officers and employees of the Federal Government who have a legitimate interest therein, and to United States citizens of known loyalty and discretion who of necessity must be informed thereof.

REQUESTS FOR PUBLICATIONS SHOULD BE ADDRESSED AS FOLLOWS:

NATIONAL ADVISORY COMMITTEE FOR AERONAUTICS
1512 H STREET, N. W.
WASHINGTON 25, D. C.

NATIONAL ADVISORY COMMITTEE
FOR AERONAUTICS
WASHINGTON
September 30, 1948

RESTRICTED

ERRATA

NACA RM No. L8G05

FULL-SCALE INVESTIGATION OF AN EQUILATERAL TRIANGULAR WING HAVING 10-PERCENT-THICK BICONVEX AIRFOIL SECTIONS

By Edward F. Whittle, Jr., and J. Calvin Lovell

September 30, 1948

Page 2: Insert the following symbol and definition between the symbols Y and N:

Z normal force (-L)

Figure 1 should be replaced with the new figure 1, a copy of which is attached.

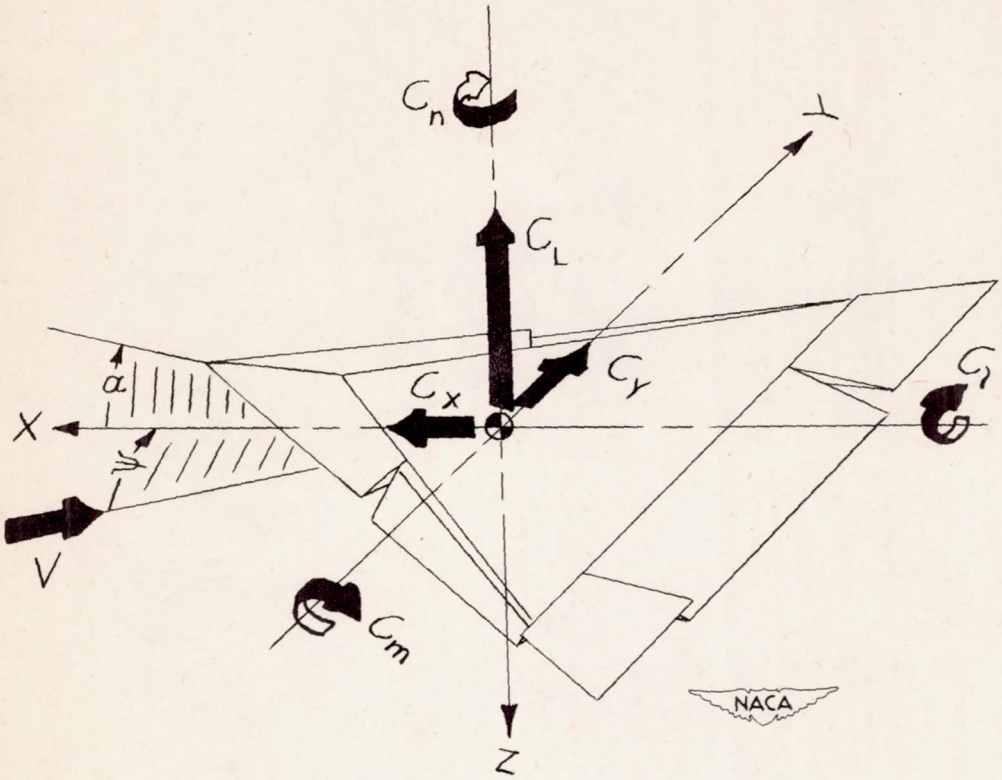

Figure 1.- The stability system of axes and sign convention for the standard NACA coefficients. All forces, force coefficients, moment coefficients, angles, and control-surface deflections are shown as positive.

NATIONAL ADVISORY COMMITTEE FOR AERONAUTICS

RESEARCH MEMORANDUM

FULL-SCALE INVESTIGATION OF AN EQUILATERAL TRIANGULAR WING HAVING 10-PERCENT-THICK BICONVEX AIRFOIL SECTIONS

By Edward F. Whittle, Jr., and J. Calvin Lovell

SUMMARY

An investigation has been made in the Langley full-scale tunnel of the low-speed characteristics of a wing having triangular plan form, 60° of sweepback at the leading edge, and 10-percent-thick biconvex airfoil sections. The investigation consisted of the determination of the effects of semispan and full-span leading-edge and trailing-edge flaps on the longitudinal aerodynamic characteristics of the wing and the effects of a vertical fin on the lateral stability characteristics.

The maximum lift coefficient of the basic triangular wing was 1.08 at a lift-drag ratio of 1.6, and both leading-edge and trailing-edge flaps were relatively ineffective in increasing the maximum lift coefficient or the lift-drag ratio. The optimum flap configuration tested had a maximum lift coefficient of 1.20 at a lift-drag ratio of 2.2. These low values of lift-drag ratio at the relatively low values of maximum lift coefficient indicate that high power-off sinking speeds will prohibit safe power-off landing of wings of this type.

The effective dihedral of the triangular wing was low, and a sizeable vertical fin did not appreciably change the effective dihedral of the wing. The basic triangular wing had a small degree of directional stability at low lift coefficients and became directionally unstable at lift coefficients above 0.90. The vertical fin contributed a stable increment of approximately -0.0012 to the directional stability throughout the lift-coefficient range.

INTRODUCTION

A wing having triangular plan form, 60° of sweepback at the leading edge, and 10-percent-thick biconvex airfoil sections has been tested in the Langley full-scale tunnel as part of a general investigation of the low-speed characteristics of probable high-speed-airplane configurations.

The investigation included tests to determine the effects of semispan and full-span leading-edge and trailing-edge flaps on the longitudinal aerodynamic characteristics of the triangular wing. Tests were made of several leading-edge and trailing-edge flap combinations to determine the optimum low-speed flap configuration. The lateral characteristics of the unflapped triangular wing, with and without a vertical fin installed, were also determined.

SYMBOLS

The data were referred to the stability axes, which are defined in figure 1. The origin of the system of axes is located at the quarter chord of the mean aerodynamic chord.

C_L	lift coefficient (L/qS)
$C_{L_{max}}$	maximum lift coefficient
C_X	longitudinal-force coefficient (X/qS)
C_D	drag coefficient (D/qS)
C_m	pitching-moment coefficient (M/qSc')
C_Y	lateral-force coefficient (Y/qS)
C_n	yawing-moment coefficient (N/qSb)
C_l	rolling-moment coefficient (L'/qSb)
L	lift
X	longitudinal force
D	drag (-X at zero yaw)
M	pitching moment about Y-axis
Y	lateral force
N	yawing moment about Z-axis
L'	rolling moment about X-axis

ρ	mass density of free-stream air
V	free-stream velocity
q	free-stream dynamic pressure $\left(\frac{\rho V^2}{2}\right)$
S	wing area
c'	mean aerodynamic chord $\left(\frac{2}{S}\int_0^{b/2} c^2\, dy\right)$
b	span of wing
α	angle of attack, degrees (measured in the plane of symmetry)
C_{L_α}	slope of lift curve, per degree
ψ	angle of yaw, degrees (positive when right wing is back)
C_{Y_ψ}	rate of change of lateral-force coefficient with angle of yaw, per degree
C_{n_ψ}	rate of change of yawing-moment coefficient with angle of yaw, per degree
C_{l_ψ}	rate of change of rolling-moment coefficient with angle of yaw, per degree
δ_f	flap deflection, degrees (positive down)
L/D	lift-drag ratio
R	Reynolds number
V_g	gliding speed, miles per hour
V_s	sinking speed, feet per second

MODEL

The triangular wing tested had a span of 23.1 feet, equilateral plan form, which corresponds to 60° of sweepback at the leading edge,

and an aspect ratio of 2.31. The airfoil sections parallel to the plane of symmetry were NACA 2S-(50)(05)-(50)(05) which are symmetrical biconvex circular-arc sections having a maximum thickness of 10 percent of the chord at the 50-percent-chord location. The wing had no geometric twist or dihedral and was made entirely of metal.

General dimensions of the triangular wing are presented in figure 2(a). The wing was provided with 12.5-percent root-chord trailing-edge plain flaps, which had the hinge line parallel to the trailing edge, and with 20-percent local-chord drooped leading-edge flaps. Sectional views of these flaps are shown in figure 2(b). The gap in the upper surface of the wing resulting from deflection of the leading-edge flaps was faired over as shown in figure 2(b). The flaps could be deflected downward as semispan inboard, semispan outboard, or full-span leading-edge or trailing-edge flaps from 0° to 60° in increments of 10°. Upward deflection of the flaps was not possible.

The vertical fin, which was installed for yaw tests, was constructed of $\frac{3}{4}$-inch plywood and strengthened by $\frac{1}{4}$-inch steel plates attached to the surface of the fin. It had an area of 29.5 square feet and an aspect ratio of 1.43. The tail boom necessary for mounting the wing in the tunnel had a 5-inch diameter and was attached to the upper surface of the wing just ahead of the trailing-edge flap. It extended approximately 5.5 feet behind the trailing edge of the wing.

Two test configurations of the triangular wing mounted in the Langley full-scale tunnel are shown in figure 3.

RESULTS AND DISCUSSION

To facilitate discussion of the results, the presentation of data is outlined below. The effect of scale is shown in figure 4 and the stalling characteristics of the triangular wing in figure 5. The effect of the various flap configurations on the longitudinal characteristics of the wing is compared with the longitudinal characteristics of the basic wing in figures 6 to 11 at a Reynolds number of approximately 6.0×10^{6}. For convenience, a summary of the maximum lift coefficients against flap deflections is presented in figure 12. In figure 13, the polar curves of three flap configurations have been superimposed on a gliding-speed and sinking-speed grid which was based on a wing loading of 40 pounds per square foot. The lateral characteristics of the yawed wing without and with a vertical fin installed are given in figures 14 and 15, respectively, and a summary of the lateral stability parameters is presented in figure 16.

No tare corrections were applied to the data, since the tares of the support-strut configuration were found to be negligible.

Jet-boundary corrections were made by an unpublished method which takes into account both the chordwise and spanwise load distribution and determines the boundary-induced downwash over the entire wing area. The conventional corrections for stream angle, buoyancy, and blocking were applied.

Longitudinal Characteristics

Basic wing.- The maximum lift coefficient of the basic triangular wing was 1.08 at an angle of attack of 32.5° and, as shown in figure 4, a variation in Reynolds number from 2.91×10^6 to 9.61×10^6 had no appreciable effect on $C_{L_{max}}$. The lift-drag ratio for the basic wing reached a maximum value of 10 at $C_L = 0.19$ and then decreased with increasing C_L to 1.6 at $C_{L_{max}}$.

Tuft studies for the basic triangular wing are given in figure 5(a). At zero lift the flow over the wing was smooth and directed rearward. As the lift coefficient increased, the vortex-type flow described in reference 1 developed over the upper surface of the wing directing the tufts toward the wing tips. This vortex action is favorable in maintaining orderly flow over the wing at the high angles of attack for maximum lift. In the region affected by the vortex action, the tufts on the left wing panel exhibited a tendency to rotate in a clockwise direction and those on the right wing panel exhibited a tendency to rotate in a counterclockwise direction. This phenomenon was previously noted for the flow over the 42° sweptback wing of reference 2. At a lift coefficient of approximately 0.50, unsteady flow developed at the wing tips, and the slope of the lift curve decreased. This region of unsteady flow, followed by an area of complete stall, moved progressively inboard with increasing lift coefficient. At the maximum lift coefficient the outboard third of the semispan appeared to be completely stalled.

The slope of the pitching-moment curve was negative and constant up to the C_L (approximately 0.50) of initial unsteady flow at the wing tips. At this C_L, the slope of the pitching-moment curve decreased somewhat but then began to increase as C_L increased. The shape of the pitching-moment curve through the stall is considered stable.

Trailing-edge flaps.- Figure 6 gives the effects of semispan inboard trailing-edge flaps on the longitudinal aerodynamic characteristics of the wing. At low lift coefficients the usual effects of trailing-edge flaps were shown, and the slope of the lift curves remained constant up to the angle of attack at which the initial unsteady flow developed at the wing tips. The pitching moment became

progressively more negative with increasing semispan flap deflection, and the breaks in the pitching-moment curves remained stable, except at a flap deflection of 60°. As shown in figure 12, the best $C_{L_{max}}$ of 1.15 obtained by semispan inboard trailing-edge flaps was at a flap deflection of 20°.

Except for flap deflections greater than 30°, the longitudinal data for full-span trailing-edge flaps are presented in figure 7. Sharp discontinuities in the lift and pitching-moment curves appeared between angles of attack of 12° and 14° (at a flap deflection of 20°, C_L decreased from 0.93 to 0.88 and C_m increased positively from -0.23 to -0.18) after which the curves proceeded at decreased slope. Discontinuities of this type were also noted in reference 3 for a triangular wing having double-wedge airfoil sections and split trailing-edge flaps. Tuft studies at a full-span trailing-edge-flap deflection of 20° (see fig. 5(b)) indicate a rapid progression of unsteady flow and stall over the wing tips between angles of attack of 12° and 14°. The largest $C_{L_{max}}$ of 1.19 for full-span trailing-edge flaps (fig. 12) was obtained at a flap deflection of 20°. The small gains in $C_{L_{max}}$ and the unstable pitching-moment breaks together with the need for outboard control surfaces render full-span trailing-edge flaps impractical for use on wings of this type.

Leading-edge flaps.- Except for flap deflections greater than 30°, figure 8 shows the effect of full-span leading-edge flaps on the longitudinal characteristics of the wing. Tuft studies of the flow over the wing with full-span leading-edge flaps deflected 20° are given in figure 5(c). The progression of spanwise flow and stall follow the same pattern as for the basic wing, although the development of the vortex-type flow was delayed somewhat by deflection of the leading-edge flaps. This delay in the vortex action is believed to be due to the decreased pressure differential between the upper and lower surfaces of the deflected flap in the immediate vicinity of the flap leading edge. The general shape of the pitching-moment curves was unaffected by leading-edge-flap deflection. However, a progressively negative shift of the curves appeared with increasing leading-edge-flap deflection, due to the alleviation of pressures and loading at the leading edge. It is shown in figure 12 that a full-span leading-edge-flap deflection of 30° produced the largest $C_{L_{max}}$ of 1.22.

The effect of deflecting the leading-edge flaps separately as semispan inboard and outboard leading-edge flaps is shown in figures 9 and 10 and their separate effect on $C_{L_{max}}$ is shown in figure 12. Deflection of the outboard leading-edge flaps improved the flow at the wing tips, thereby providing more linear pitching-moment curves as compared to the pitching-moment curves for the basic wing. However,

the maximum lift coefficient was increased only to 1.16 at the excessively large flap angle of 50°. Separate deflection of the semispan inboard leading-edge flaps had an adverse effect on $C_{L_{max}}$. The general shape of the pitching-moment curves was unaffected by flap deflection, but they were shifted progressively in the negative direction due to loss in lift at the wing apex.

Flap combinations.- The effect of three leading-edge and trailing-edge flap combinations on the longitudinal characteristics of the wing is given in figure 11. Flap deflections of 20° were used throughout. The deflection of full-span leading-edge flaps and semispan inboard trailing-edge flaps had no appreciable effect on $C_{L_{max}}$ or L/D at $C_{L_{max}}$, but the pitching-moment curve was shifted in a negative direction. The addition to this flap combination of outboard trailing-edge flaps shifted the lift curve upward to a $C_{L_{max}}$ of 1.20, at which L/D was 1.5, and the pitching-moment curve was shifted still more in a negative direction.

The deflection of semispan outboard leading-edge flaps in conjunction with semispan inboard trailing-edge flaps extended the linearity of the lift curve, thereby resulting in the maximum lift coefficient at an angle of attack of 25.5° as compared with 32.5° for the basic wing. The value of $C_{L_{max}}$ was increased to 1.20, and the lift-drag ratio at $C_{L_{max}}$ was increased to 2.2. This combination produced the most linear pitching-moment characteristics with a less negative shift of the curve though the break at the stall was marginal. The combination of outboard leading-edge flaps and inboard trailing-edge flaps is considered the optimum landing configuration tested.

Figure 13 gives the polar curves for several flap configurations superimposed on a gliding-speed and sinking-speed grid based on an assumed wing loading of 40 pounds per square foot. The curve for the optimum flap combination tested shows that the power-off sinking speed at the estimated lift coefficient (0.77) for the landing approach is 49 feet per second at a flight speed of 143 miles per hour. It is believed that this high power-off sinking speed will prohibit safe power-off landings.

Lateral Characteristics

The variations of the lateral stability parameters C_{l_ψ}, C_{n_ψ}, and C_{Y_ψ} with C_L in figure 16 were obtained from the variations of C_l, C_n, and C_Y with ψ (figs. 14 and 15) at small angles of yaw ($\psi = \pm 2°$). Since the stability boundaries for a triangular wing have not been

established, there is some question as to the significance of the magnitude of the stability parameters. In general, however, it is believed that positive values of C_{l_ψ} and negative values of C_{n_ψ} are necessary for satisfactory flying qualities.

The value of C_{l_ψ} for the basic triangular wing increased from zero at zero lift to a maximum value of 0.0012 at $C_L = 0.40$; and as C_L increased above 0.40, C_{l_ψ} decreased, reaching zero at $C_L = 0.64$ and -0.004 at a C_L of 1.00. The vertical fin had no appreciable effect on the effective dihedral. It is believed that deflection of the outboard leading-edge flaps would extend the lift-coefficient range for positive effective dihedral, since these flaps improve the flow at the wing tips.

The basic triangular wing had a small degree of directional stability at lift coefficients between 0.20 and 0.90. The minimum value of C_{n_ψ} for the basic wing was -0.0007 at a C_L of 0.80, and at lift coefficients above this value C_{n_ψ} increased with C_L to positive values at lift coefficients above 0.92. The vertical fin contributed a stable increment of approximately -0.0012 to C_{n_ψ} throughout the lift-coefficient range but did not prevent C_{n_ψ} from becoming positive above $C_L = 1.0$. These values of C_{n_ψ} for the fin-on configuration are believed to be adequate for satisfactory flying qualities.

The basic triangular wing had a small degree of lateral-force effect at low lift coefficients, due to asymmetry of the model and/or air stream. At lift coefficients above 0.60, C_{Y_ψ} increased with C_L to 0.004 at a C_L of 1.00. The vertical fin contributed an increment of approximately 0.005 to C_{Y_ψ} throughout the C_L range.

CONCLUSIONS

The results of tests at a high Reynolds number of a triangular wing having 10-percent-thick biconvex airfoil sections indicate the following conclusions:

1. Since the optimum flap configuration tested (inboard semispan trailing-edge and outboard semispan leading-edge flaps deflected 20°) only increased $C_{L_{max}}$ to 1.20, it is believed that the maximum lift coefficient of an equilateral triangular wing having plain trailing-edge flaps and drooped leading-edge flaps will be relatively low.

2. Low values of lift-drag ratio, at the relatively low values of maximum lift coefficient, indicate that high power-off sinking speeds will prohibit safe power-off landing of wings of this type.

3. Semispan outboard leading-edge flaps in combination with the semispan inboard trailing-edge flap gave the most linear pitching-moment variation of those combinations tested. Although the marginal break at the stall is not a desirable one, it is believed that no serious stalling characteristics due to this condition will be encountered in flight. The linearity of the pitching-moment curves and generally stable tendencies through the stall indicate that triangular wings of the type tested can be designed to have satisfactory low-speed longitudinal stability characteristics.

4. The effective dihedral of the triangular wing was low at low lift coefficients $\left(\text{maximum } C_{l_\psi} \text{ was } 0.0012 \text{ at a } C_L \text{ of } 0.40\right)$ and became negative at lift coefficients above 0.63. A vertical fin having 13 percent of the wing area and an aspect ratio of 1.43 did not appreciably change the effective dihedral of the wing. It is believed that deflection of the outboard leading-edge flaps would extend the lift-coefficient range for positive effective dihedral.

5. The basic triangular wing had a small degree of directional stability at low lift coefficients and became directionally unstable at lift coefficients above 0.90. The vertical fin contributed a stable increment of approximately -0.0012 to C_{n_ψ} throughout the lift-coefficient range.

Langley Aeronautical Laboratory
National Advisory Committee for Aeronautics
Langley Field, Va.

REFERENCES

1. Wilson, Herbert A., Jr., and Lovell, J. Calvin: Full-Scale Investigation of the Maximum Lift and Flow Characteristics of an Airplane Having Approximately Triangular Plan Form. NACA RM No. L6K20, 1946.

2. Neely, Robert H., and Conner, D. William: Aerodynamic Characteristics of a 42° Swept-Back Wing with Aspect Ratio 4 and NACA 64_1-112 Airfoil Sections at Reynolds Numbers from 1,700,000 to 9,500,000. NACA RM No. L7D14, May 23, 1947.

3. Anderson, Adrien E.: An Investigation at Low Speed of a Large-Scale Triangular Wing of Aspect Ratio Two. - I. Characteristics of a Wing Having a Double-Wedge Airfoil Section with Maximum Thickness at 20-Percent Chord. NACA RM No. A7F06, 1947.

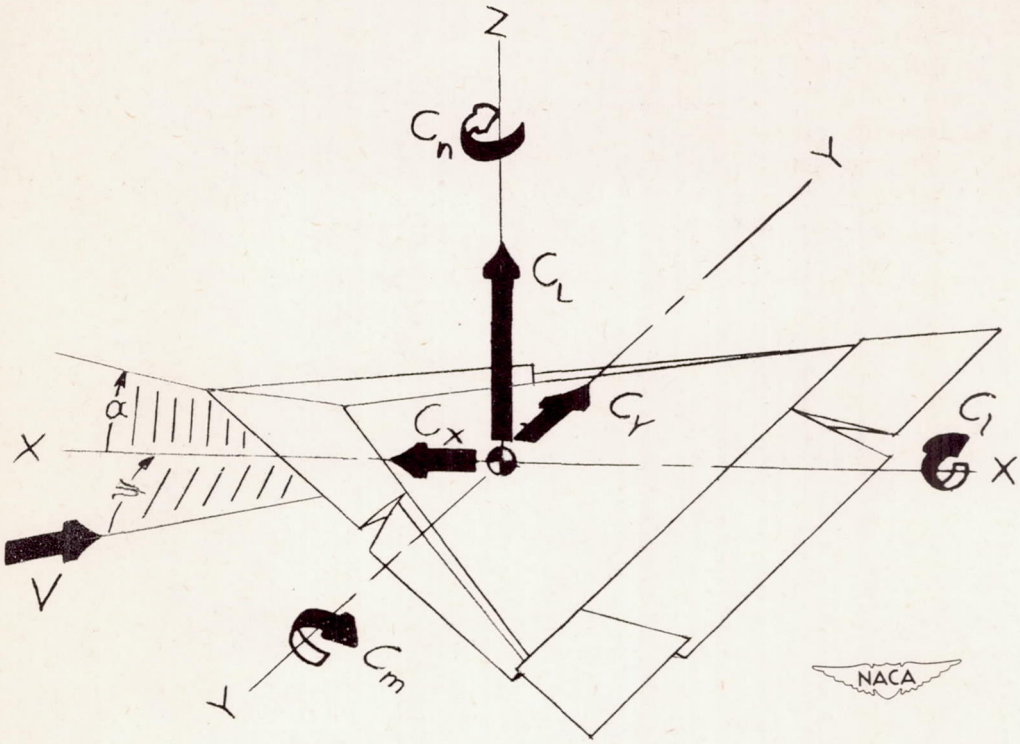

Figure 1.- The stability system of axes and sign convention for the standard NACA coefficients. All force coefficients, moment coefficients, angles, and control-surface deflections are shown as positive.

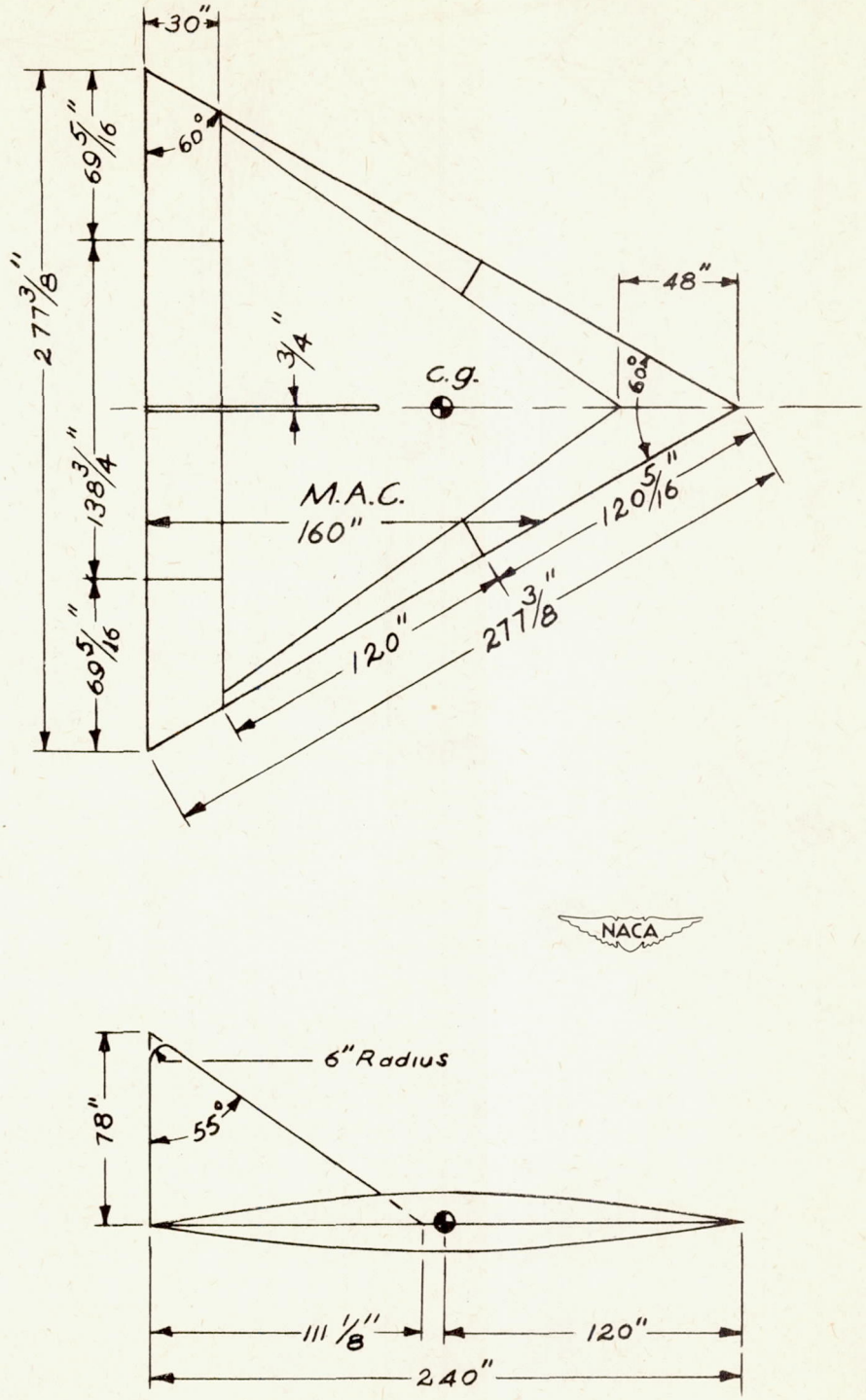

(a) Dimensions of the triangular wing.

Figure 2.- General arrangement of the low-aspect-ratio triangular wing.

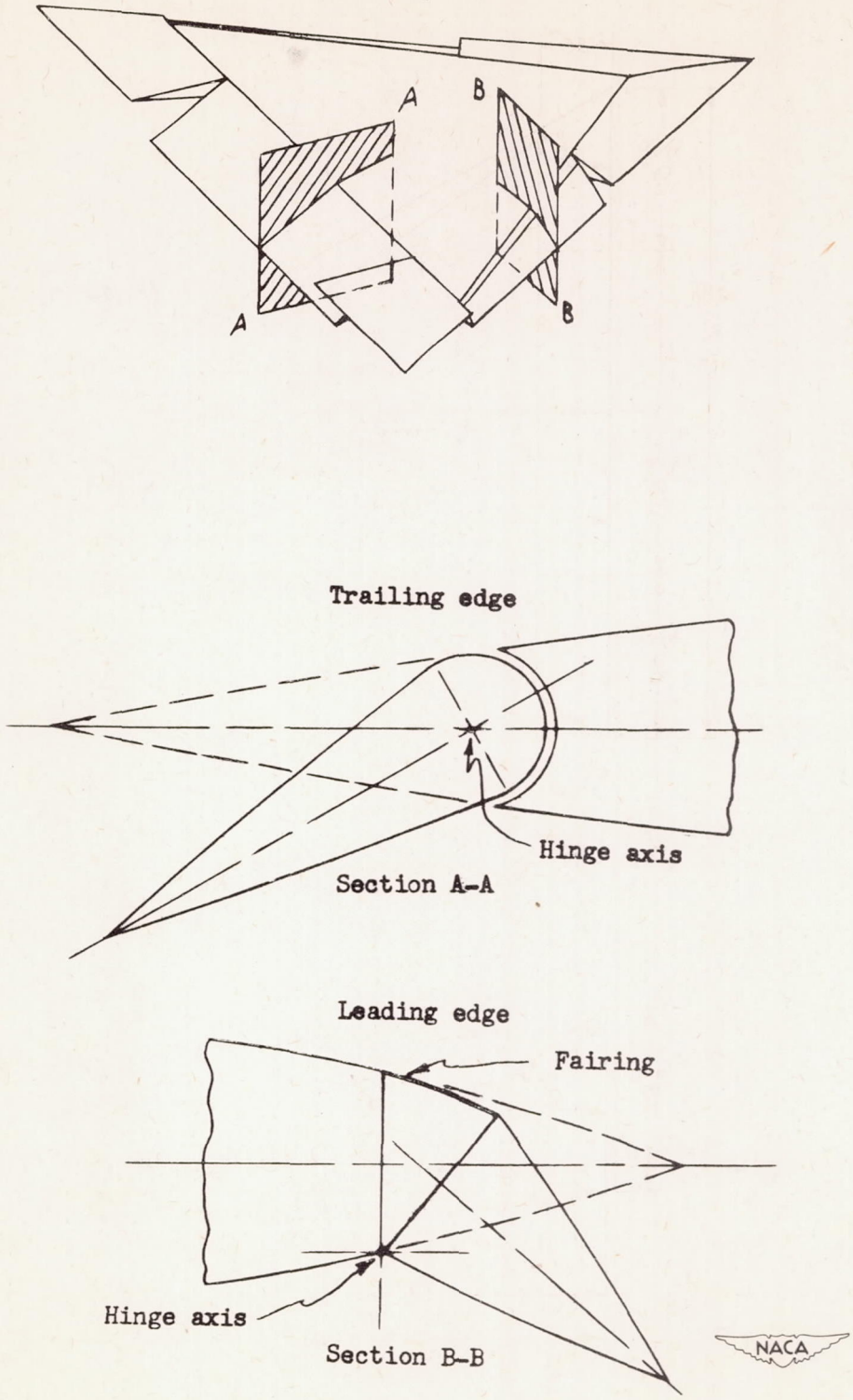

(b) Sectional views of the triangular-wing flaps.

Figure 2.- Concluded.

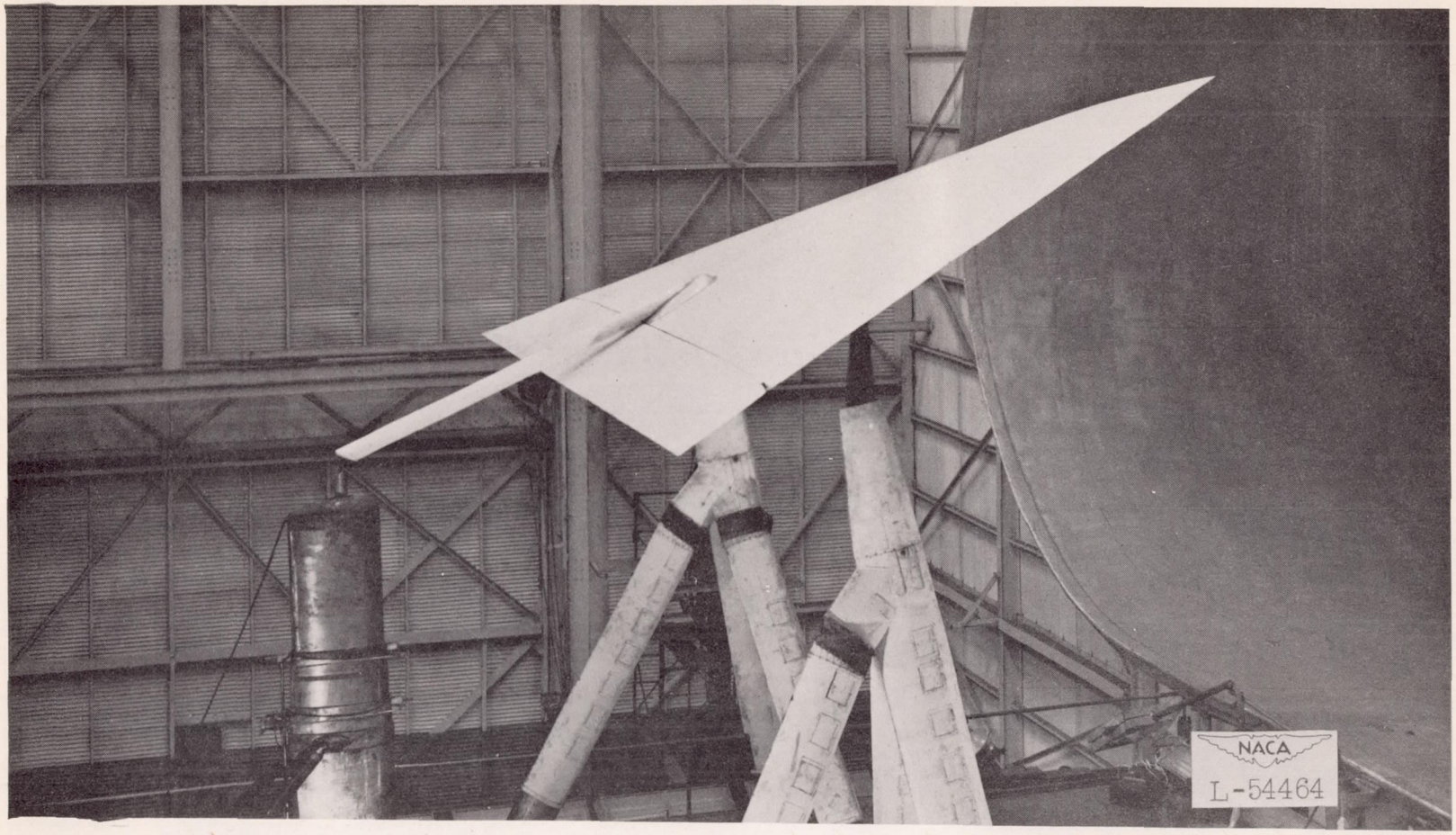

(a) Basic wing.

Figure 3.- The low-aspect-ratio triangular wing mounted in the Langley full-scale tunnel.

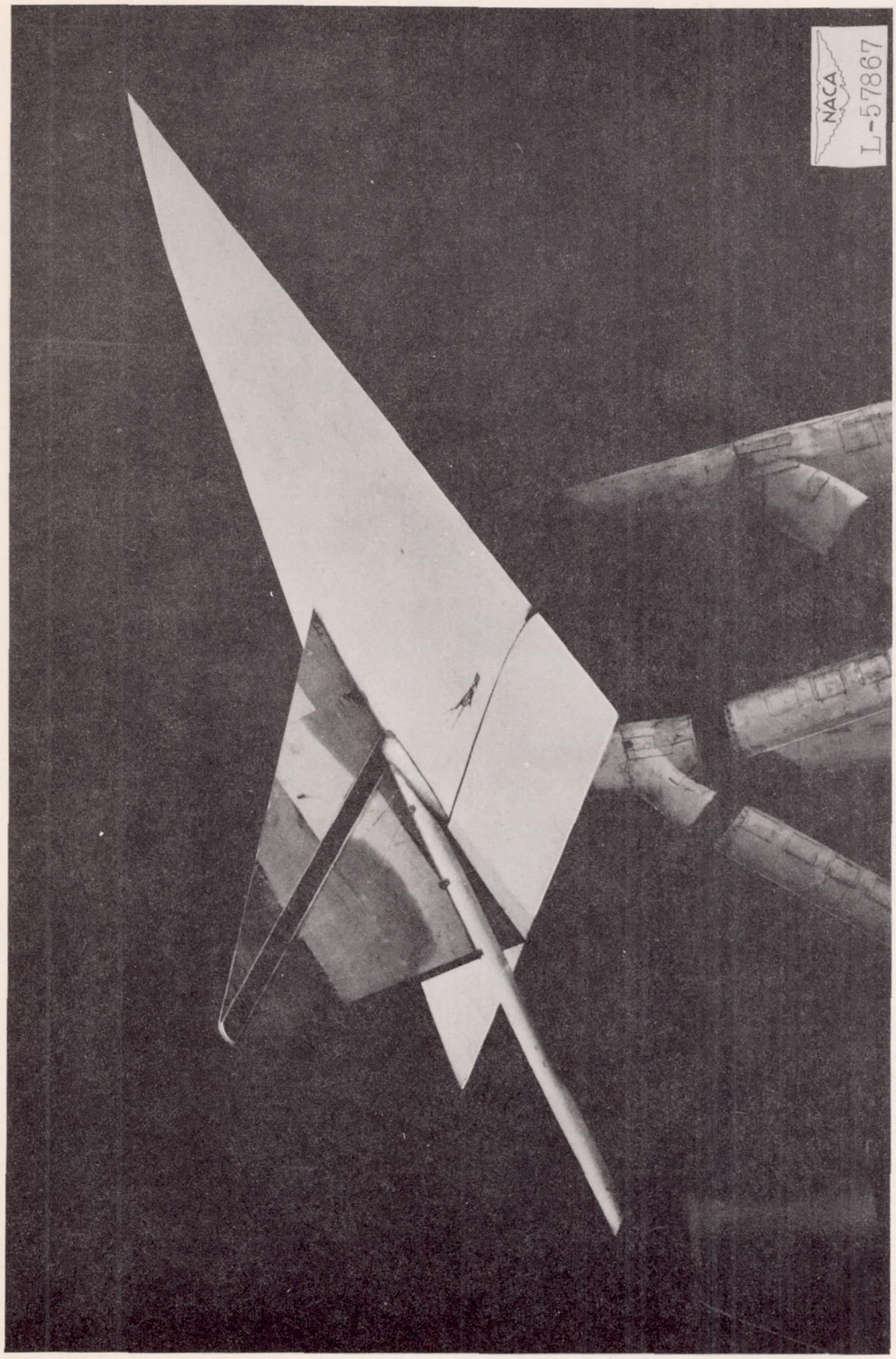

(b) Vertical fin installed for yaw tests.

Figure 3.- Concluded.

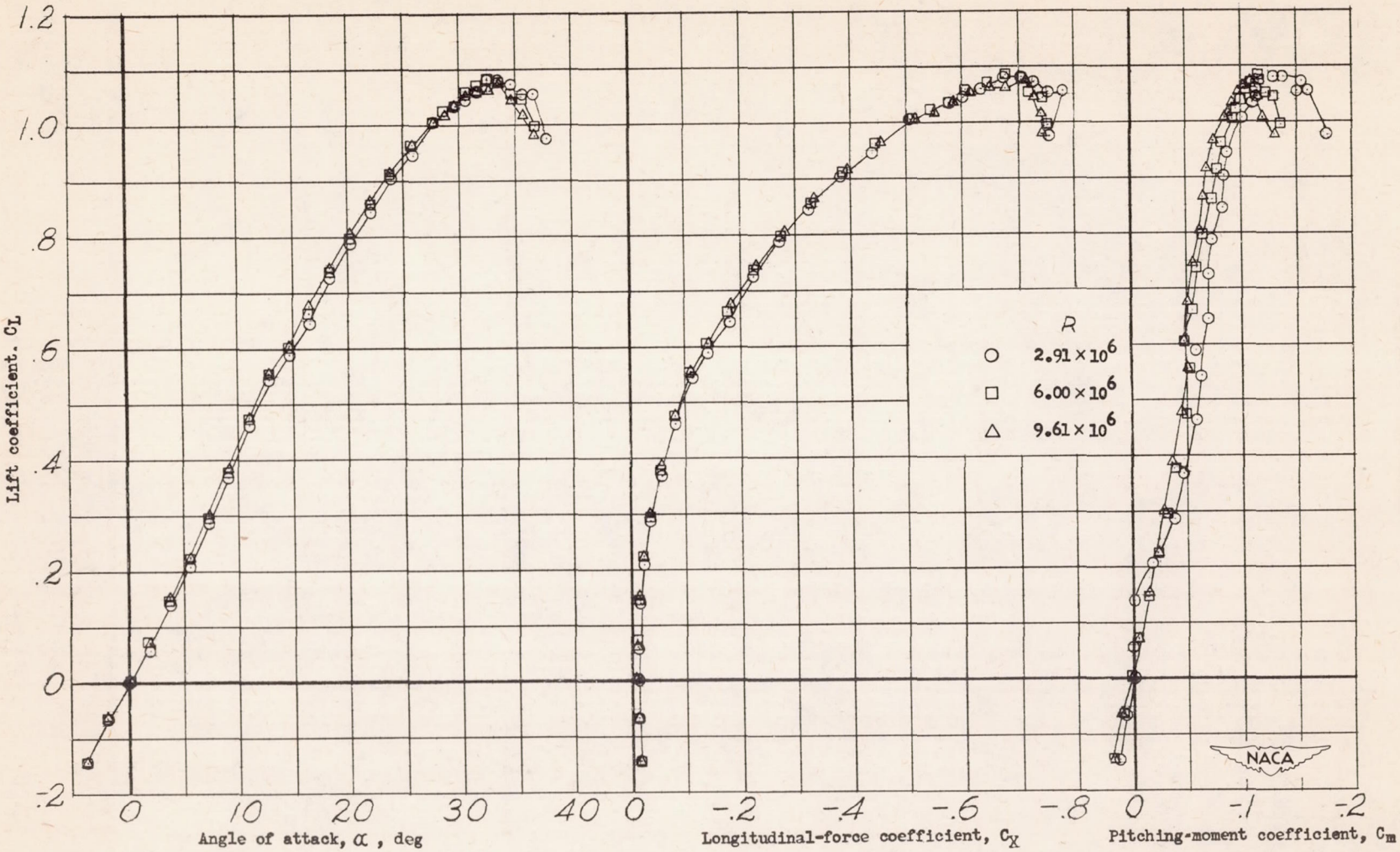

Figure 4.- Effect of Reynolds number on the aerodynamic characteristics of the triangular wing.

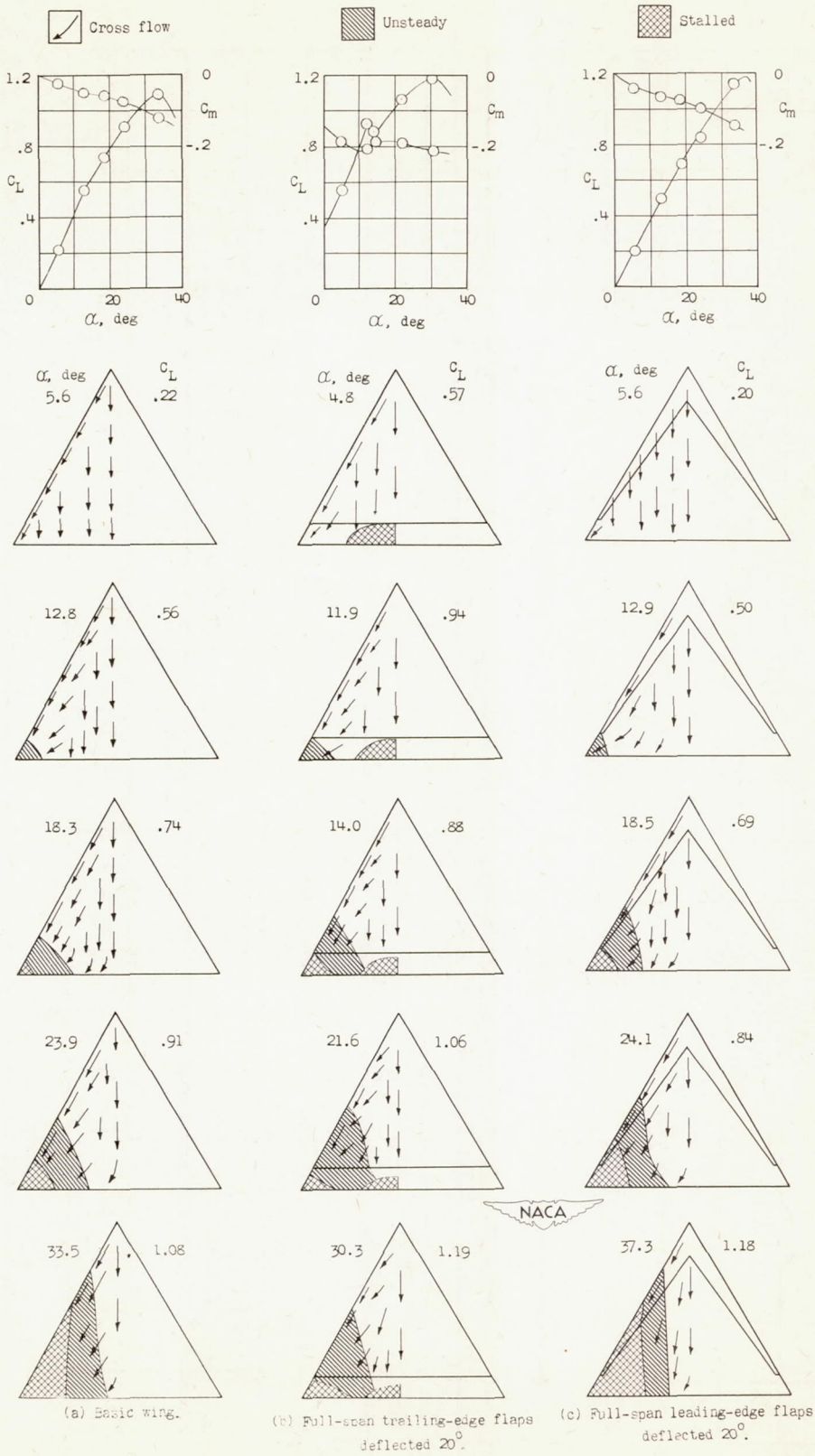

(a) Basic wing.

(b) Full-span trailing-edge flaps deflected 20°.

(c) Full-span leading-edge flaps deflected 20°.

Figure 5.- Stalling characteristics of the triangular wing.

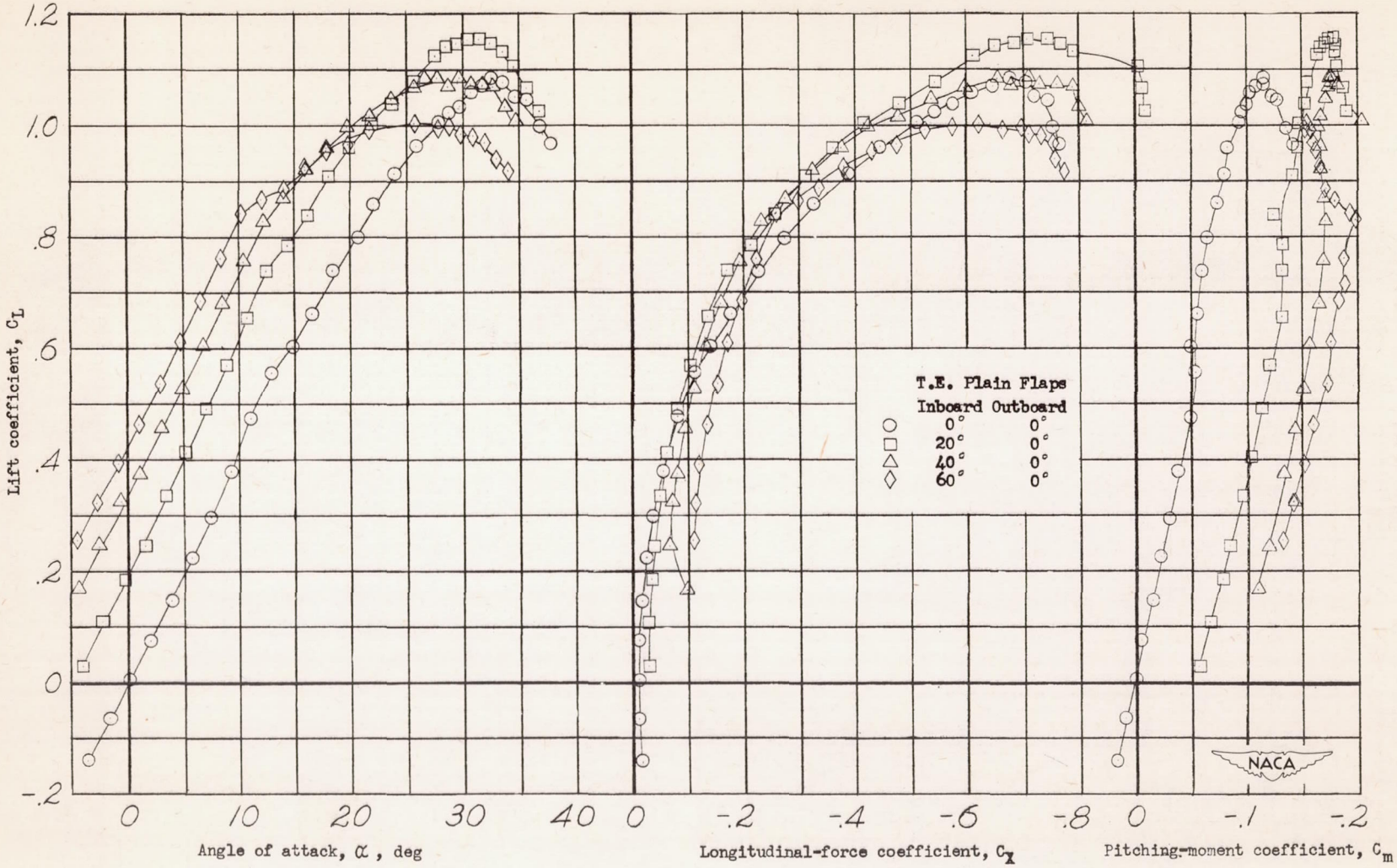

Figure 6.- Effect of semispan inboard trailing-edge-flap deflection on the aerodynamic characteristics of the triangular wing. $\psi = 0^{\circ}$.

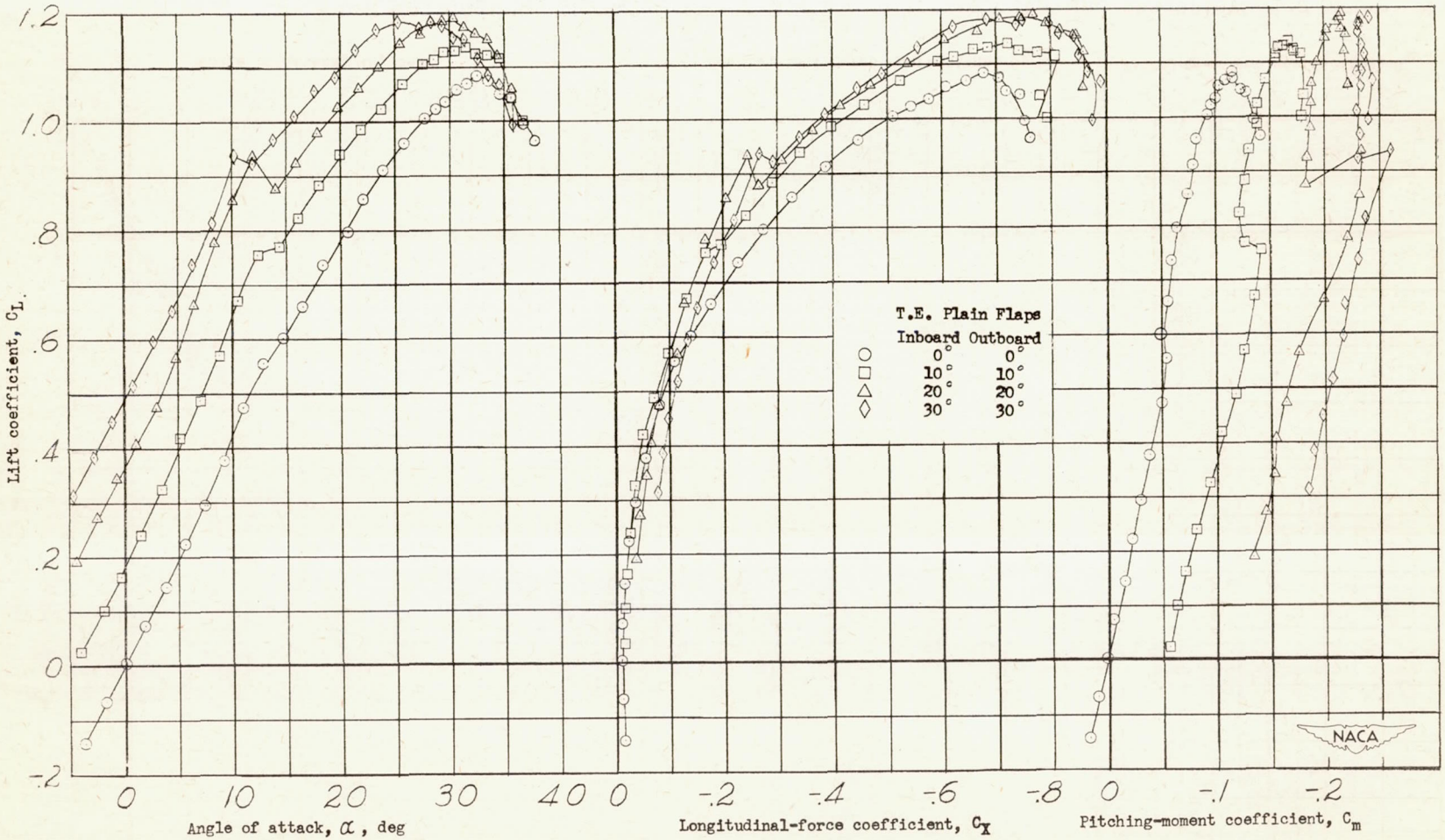

Figure 7.- Effect of full-span trailing-edge-flap deflection on the aerodynamic characteristics of the triangular wing. $\psi = 0^{\circ}$.

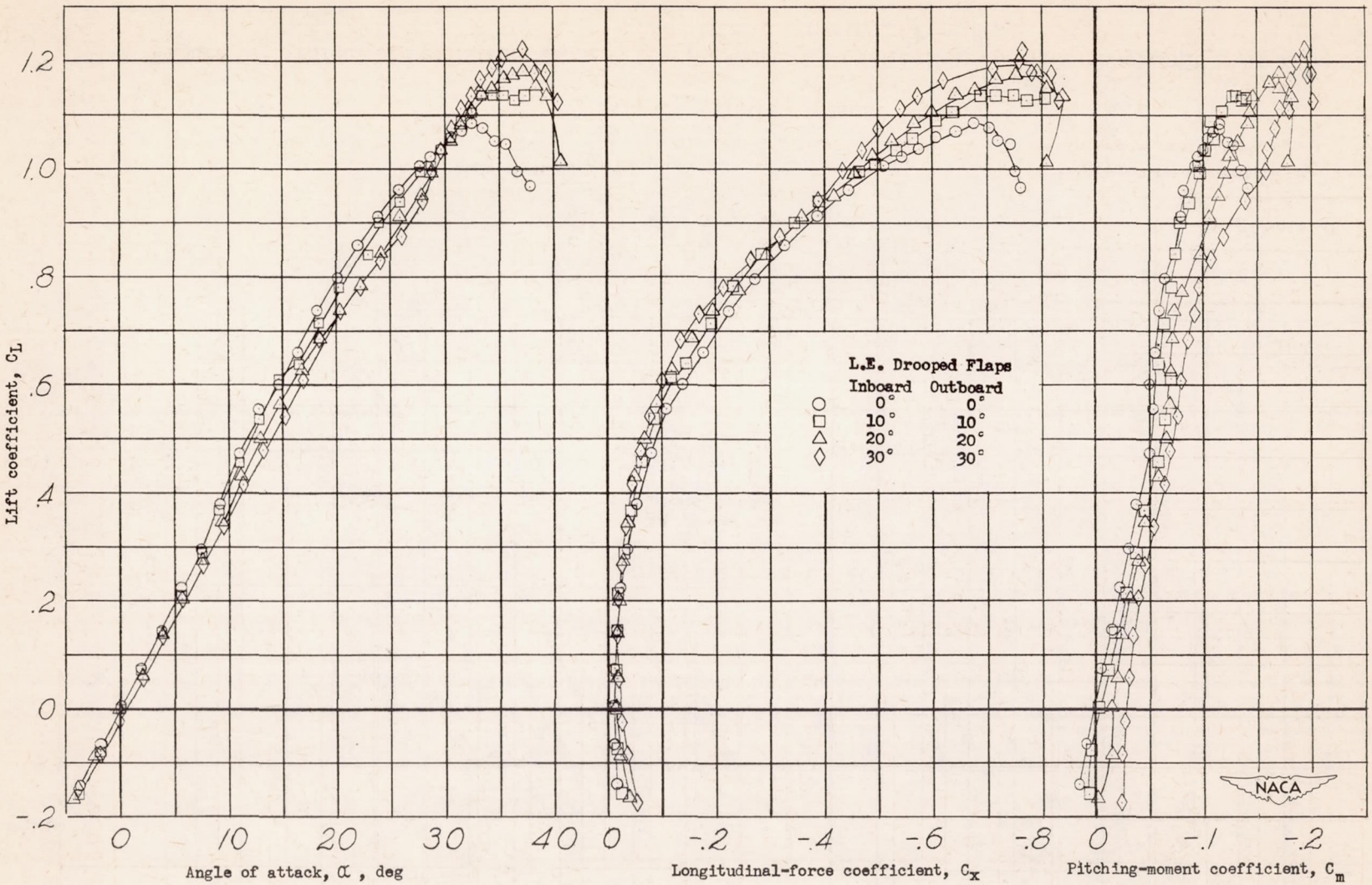

Figure 8.- Effect of full-span leading-edge-flap deflection on the aerodynamic characteristics of the triangular wing. $\psi = 0^{\circ}$.

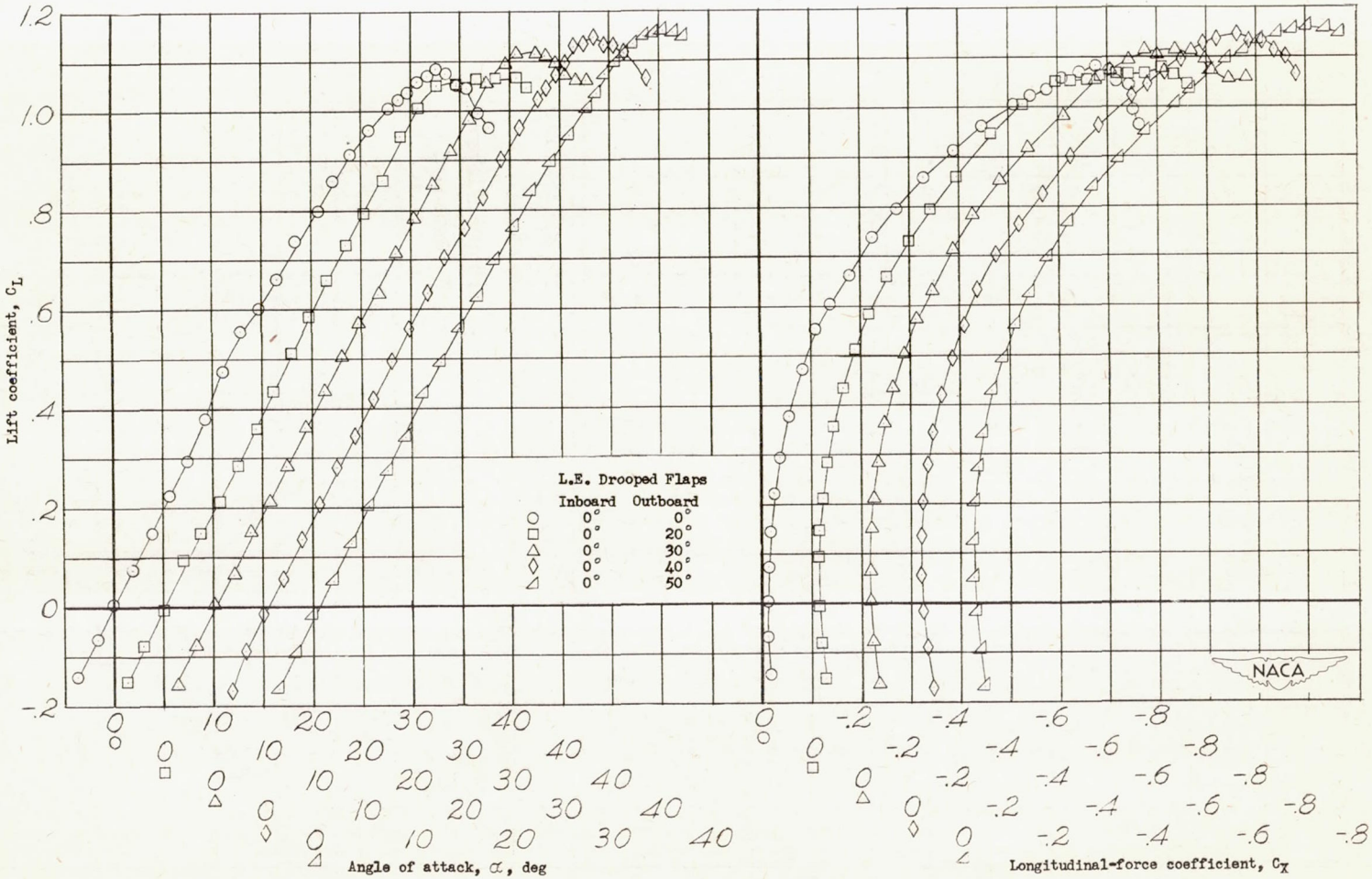

(a) C_L plotted against α and C_X.

Figure 9.- Effect of semispan outboard leading-edge-flap deflection on the aerodynamic characteristics of the triangular wing. $\psi = 0^{\circ}$.

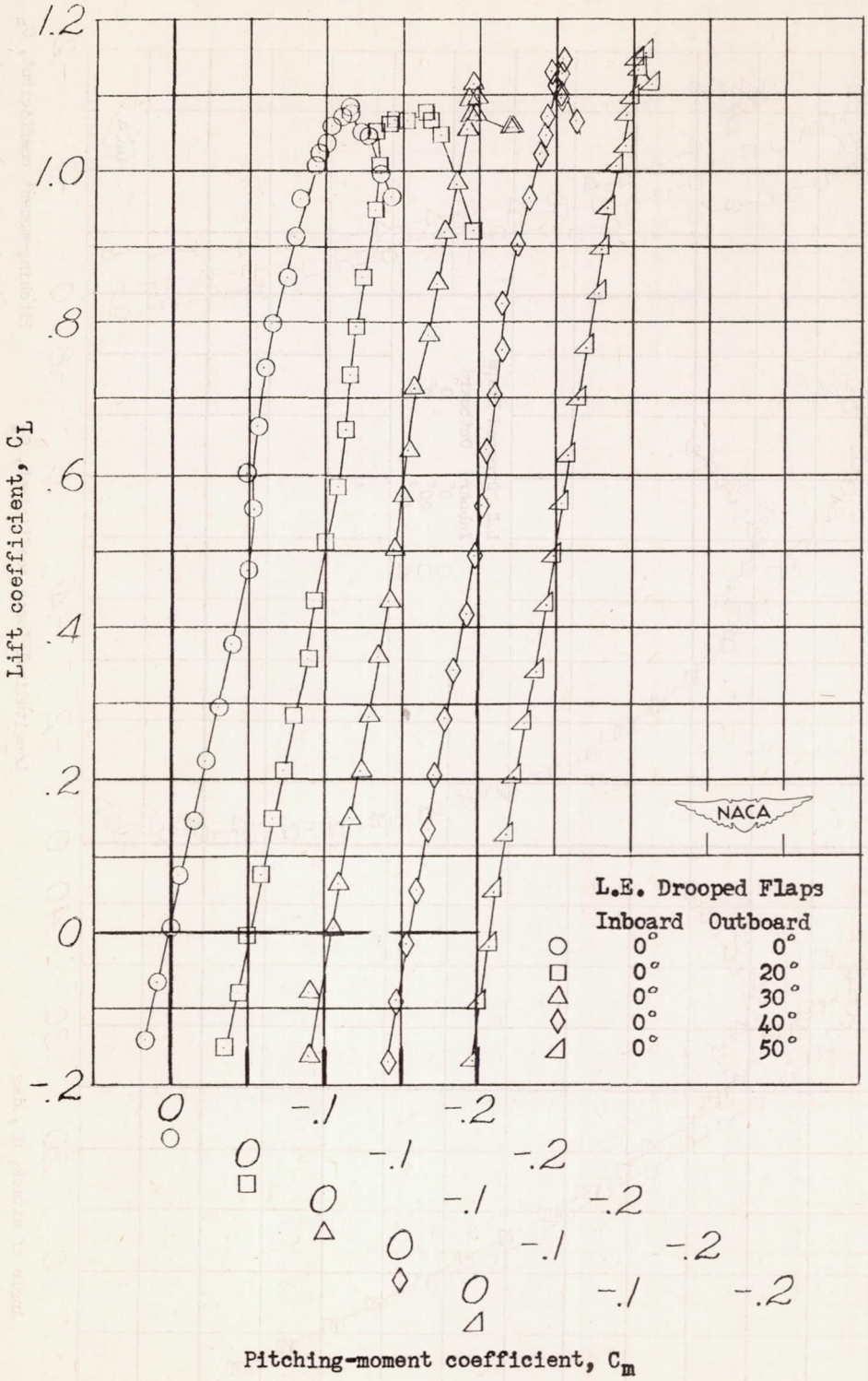

(b) C_L plotted against C_m.

Figure 9.- Concluded.

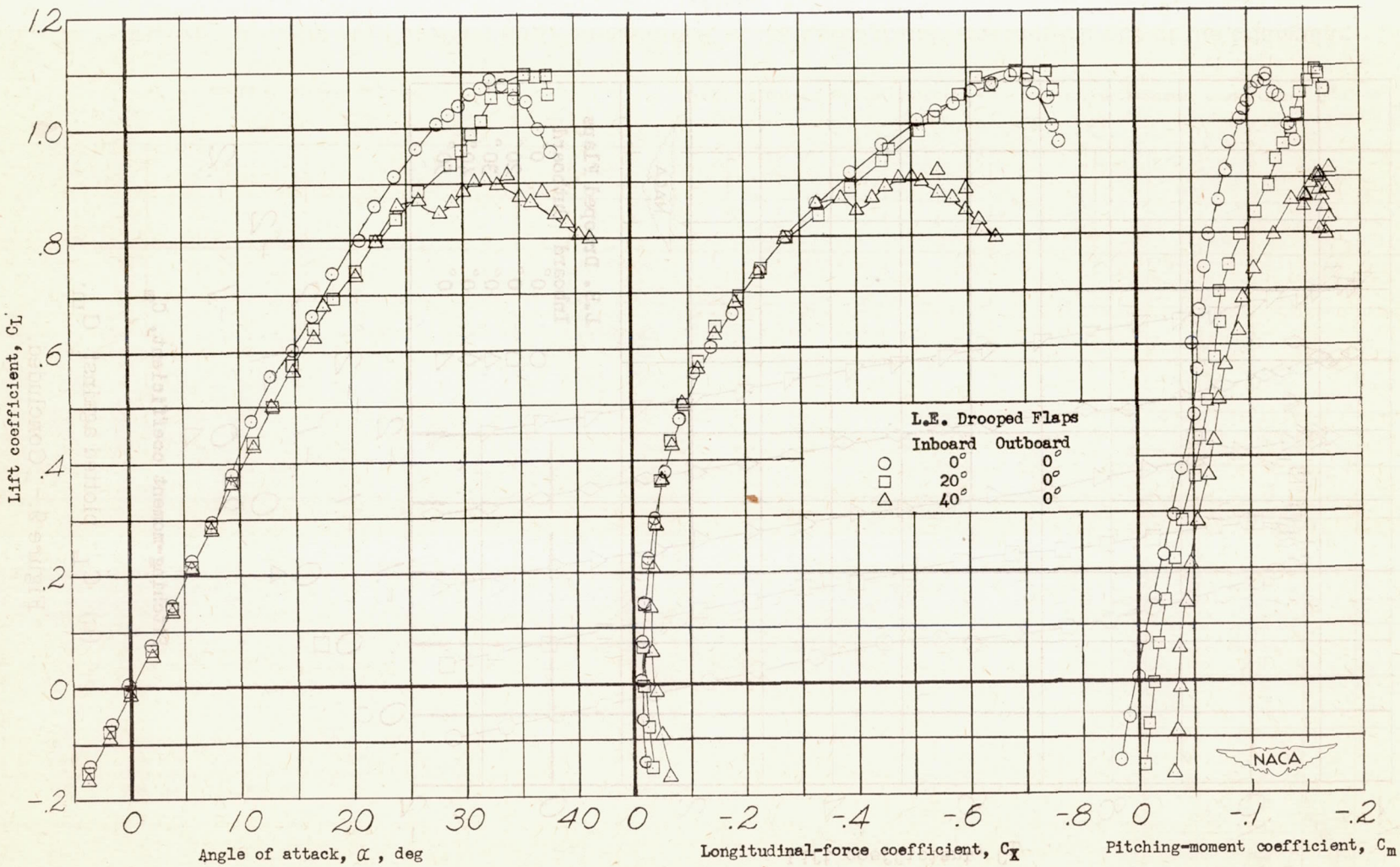

Figure 10.- Effect of semispan inboard leading-edge-flap deflection on the aerodynamic characteristics of the triangular wing. $\psi = 0^{\circ}$.

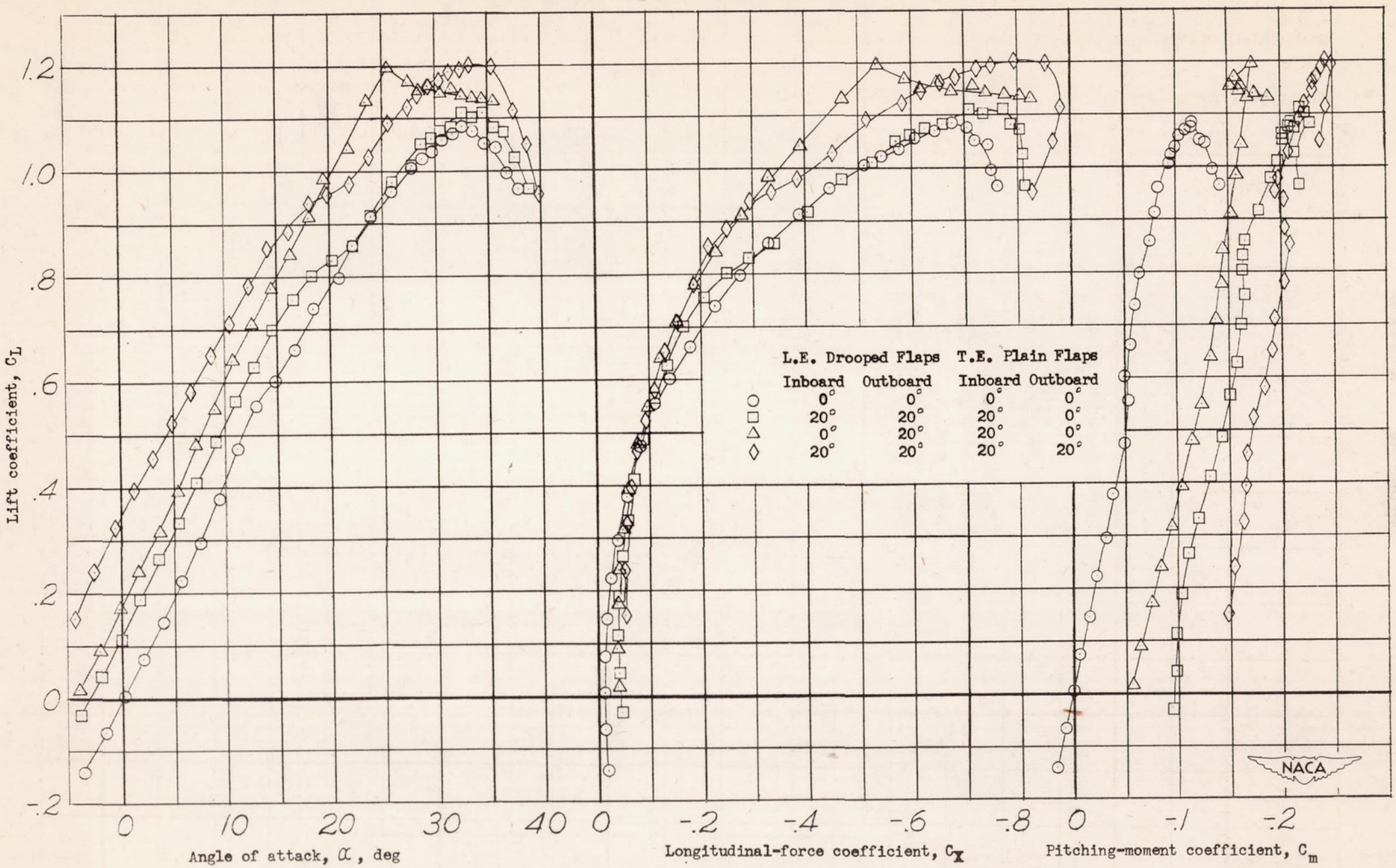

Figure 11.- Effect of various flap combinations on the aerodynamic characteristics of the triangular wing. $\psi = 0^{\circ}$.

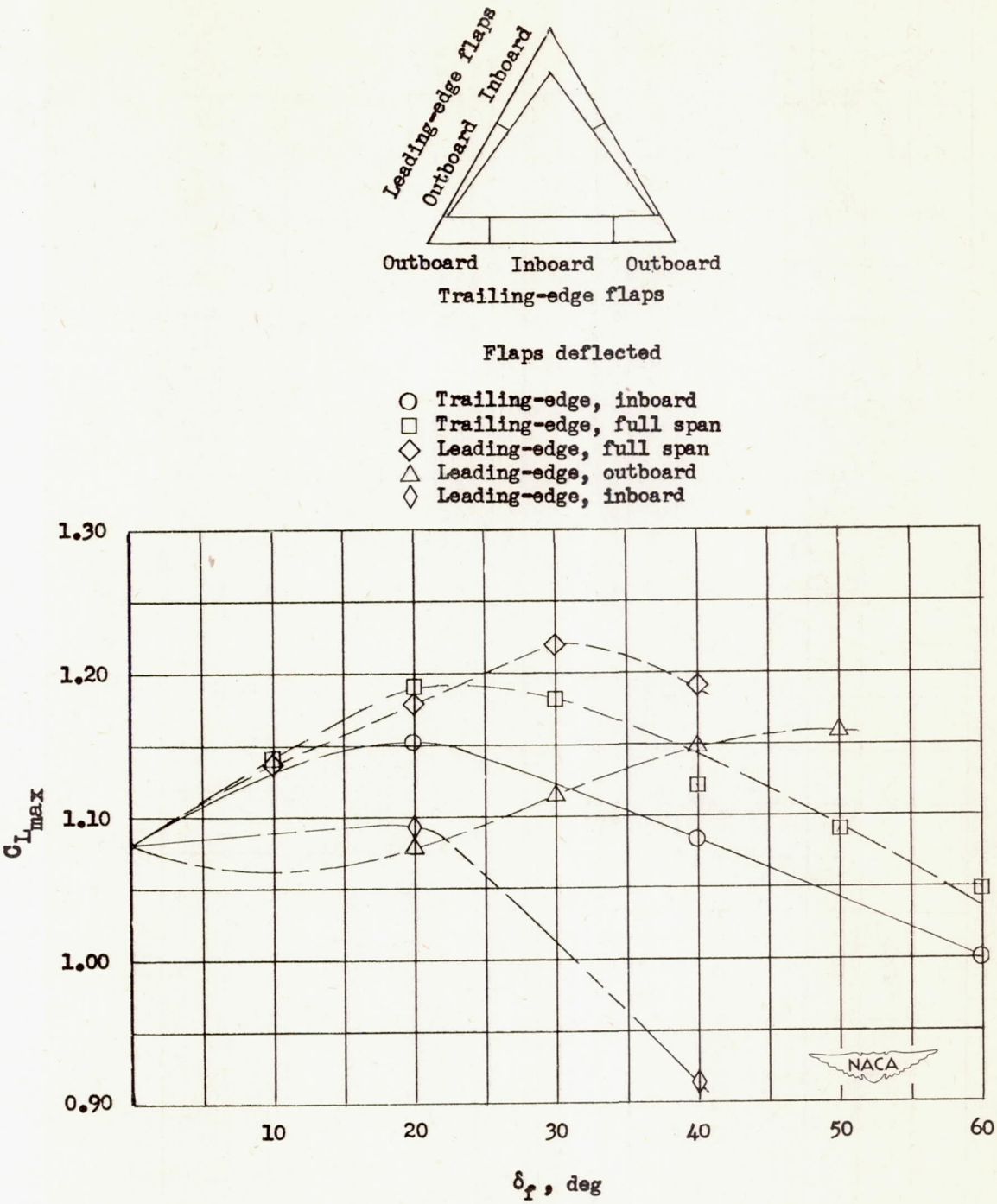

Figure 12.- Effect of flaps on the maximum lift coefficient.

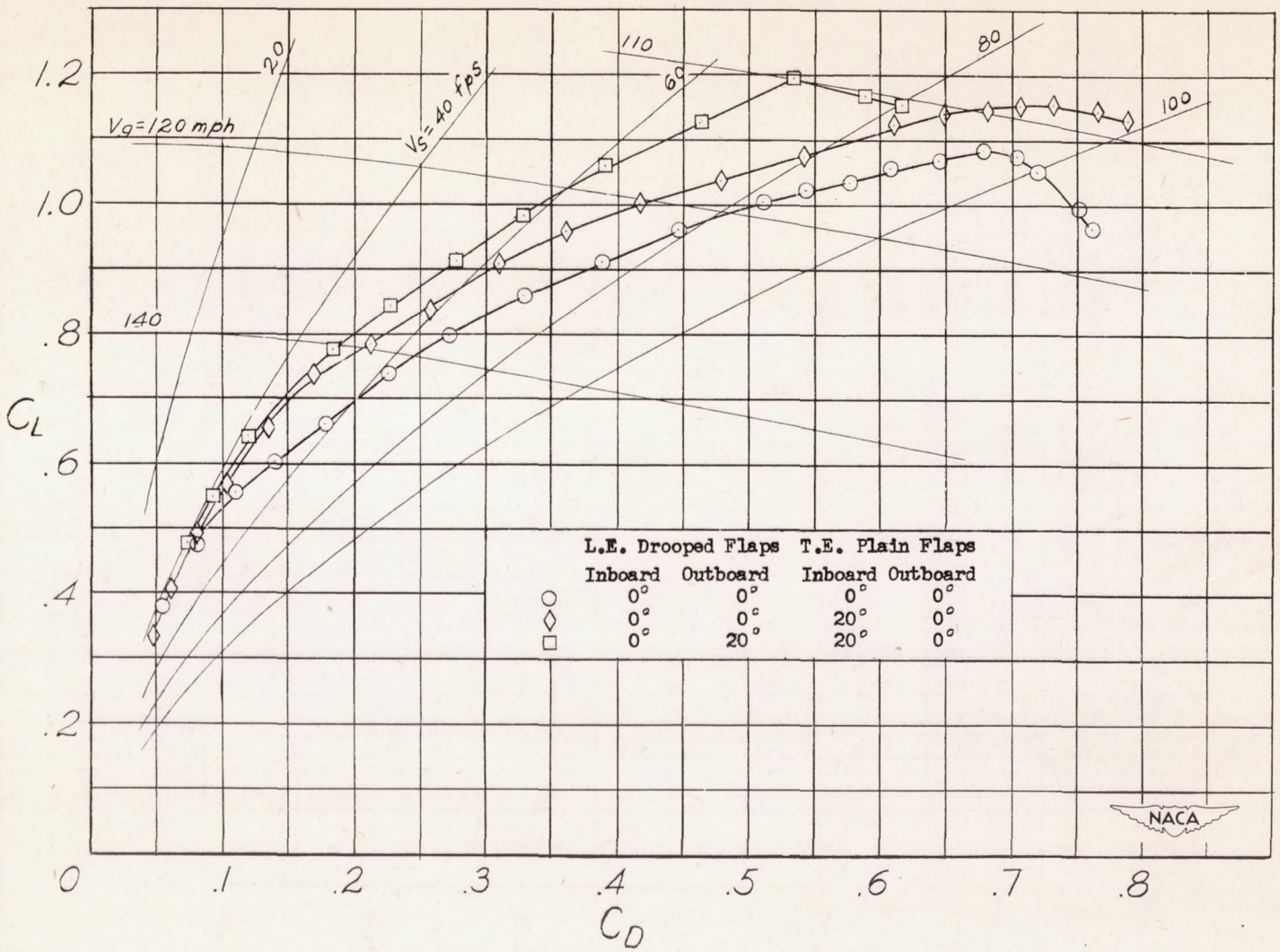

Figure 13.- Gliding speed and sinking speed of the triangular wing with the various flap combinations and a wing loading of 40 pounds per square foot.

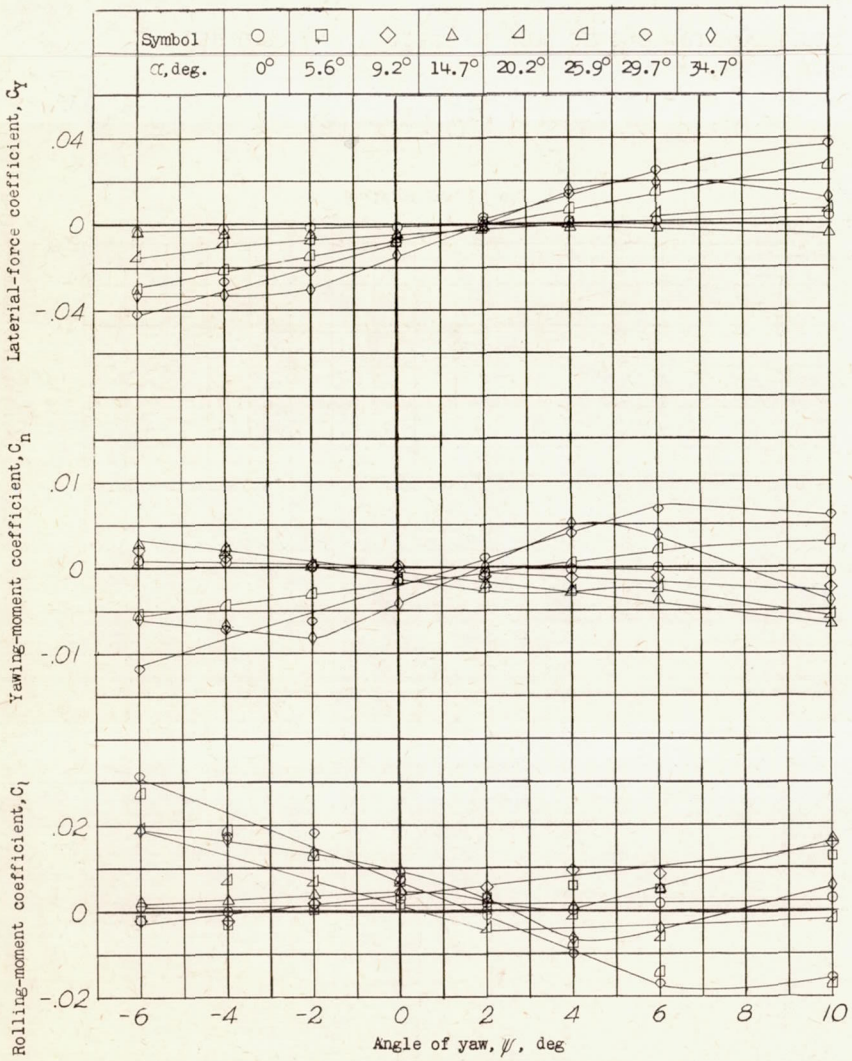

(a) C_Y; C_n; C_l.

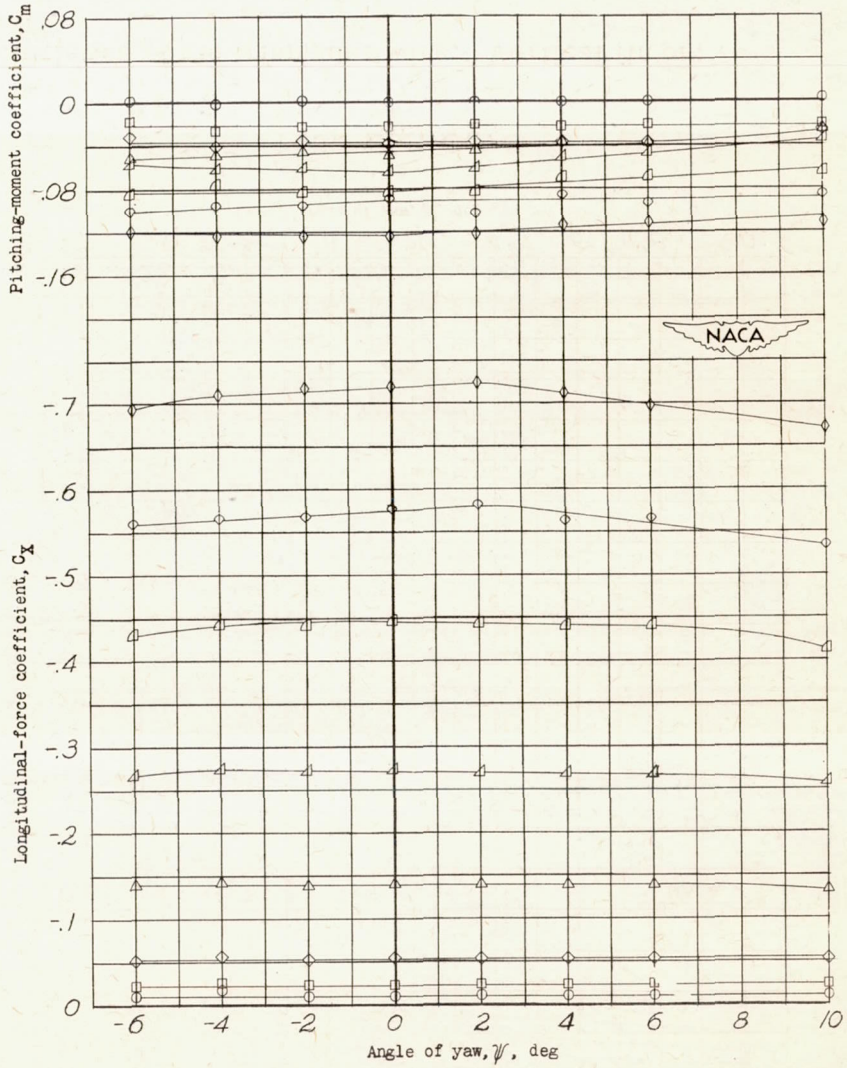

(b) C_m; C_X.

Figure 14.- Effect of yaw on the aerodynamic characteristics of the triangular wing. Vertical fin off; $\delta_f = 0^\circ$.

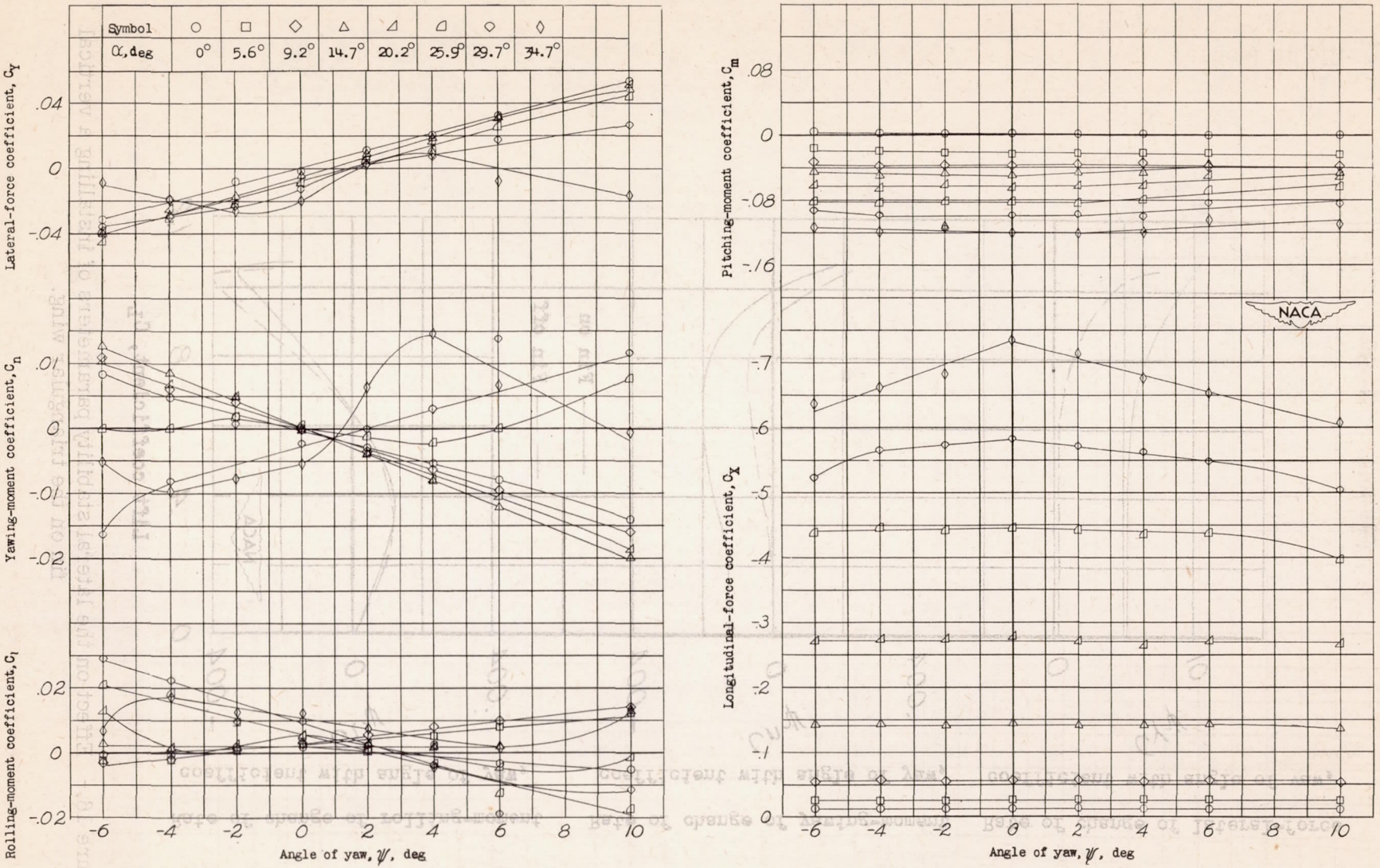

(a) C_Y; C_n; C_l.

(b) C_m; C_X.

Figure 15.- Effect of yaw on the aerodynamic characteristics of the triangular wing. Vertical fin on; $\delta_f = 0^\circ$.

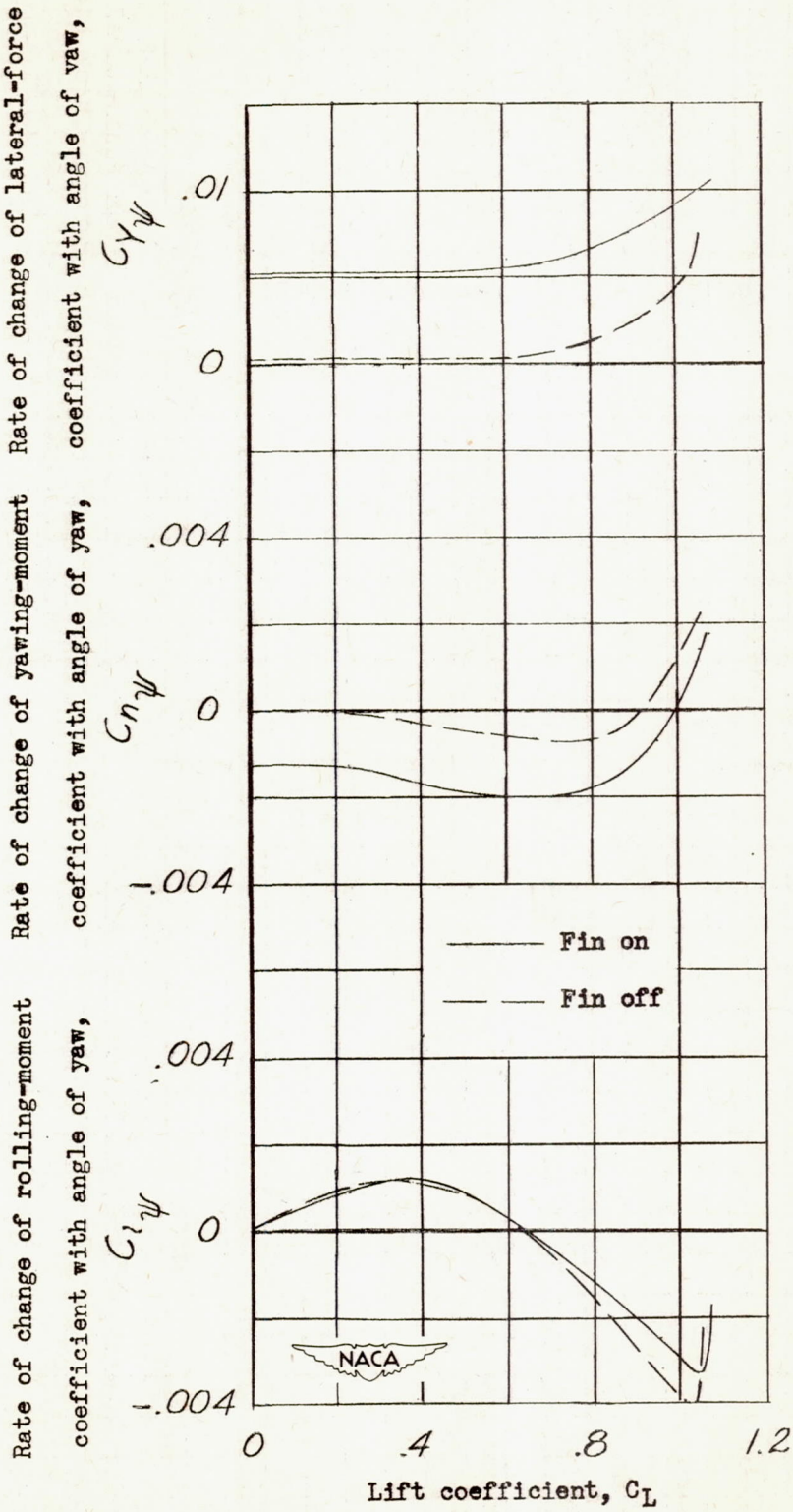

Figure 16.- Effect on the lateral stability parameters of installing a vertical fin on the triangular wing.